

Project 1

Quantum Optics Group 3
Hayden McGuinness, Anthony Clark, Anika Pflanzner

18 April 2007

1 Problem 1

In this problem we investigate the interaction of a two-state atom with a classical field. In this semiclassical regime, the evolution of the quantum state of the atom is determined by the two-state optical Bloch equations. Solutions to these equations are obtained numerically for various representative combinations of the relevant physical parameters with a program written in Fortran 95, and plots of the excited state population are presented. In cases where analytic solutions can be obtained, we have compared these to the numerical solutions, with the results presented as plots of the difference of the numerical from the analytic.

1.1 Theoretical background

The Bloch equations can be written in terms of matrix elements of the density operator as:

$$\begin{aligned}\partial_t \rho_{ee} &= i\frac{\Omega}{2}(\tilde{\rho}_{eg} - \tilde{\rho}_{ge}) - \Gamma\rho_{ee} \\ \partial_t \rho_{gg} &= -i\frac{\Omega}{2}(\tilde{\rho}_{eg} - \tilde{\rho}_{ge}) + \Gamma\rho_{ee} \\ \partial_t \tilde{\rho}_{ge} &= -(\gamma_{\perp} + i\Delta)\tilde{\rho}_{ge} - i\frac{\Omega}{2}(\rho_{ee} - \rho_{gg}) \\ \partial_t \tilde{\rho}_{eg} &= -(\gamma_{\perp} - i\Delta)\tilde{\rho}_{eg} + i\frac{\Omega}{2}(\rho_{ee} - \rho_{gg}),\end{aligned}\tag{1}$$

where Ω is the Rabi frequency, Δ the detuning and

$$\gamma_{\perp} = \frac{\Gamma}{2} + \gamma_c\tag{2}$$

is the transverse decay rate, where γ_c represents the broadening due to collisions. In this case we assume homogeneous broadening and therefore $\gamma_c = 0$, so

$$\gamma_{\perp} = \frac{\Gamma}{2}.\tag{3}$$

Together with the normalization condition,

$$\rho_{ee} + \rho_{gg} = 1, \quad (4)$$

these determine the time evolution of the quantum state.

It is convenient to rewrite $\tilde{\rho}_{eg}$ and $\tilde{\rho}_{ge}$ in terms of the real-valued components of the Bloch vector, given by:

$$\begin{aligned} \langle \sigma_x \rangle &= \tilde{\rho}_{eg} + \tilde{\rho}_{ge} \\ \langle \sigma_y \rangle &= i(\tilde{\rho}_{eg} - \tilde{\rho}_{ge}) \end{aligned} \quad (5)$$

Doing this, and using the normalization condition to eliminate the ground state population, ρ_{gg} , the equations of motion become:

$$\begin{aligned} \partial_t \rho_{ee} &= \frac{\Omega}{2} \langle \sigma_y \rangle - \Gamma \rho_{ee} \\ \partial_t \langle \sigma_x \rangle &= \Delta \langle \sigma_y \rangle - \Gamma \langle \sigma_x \rangle \\ \partial_t \langle \sigma_y \rangle &= -\Delta \langle \sigma_x \rangle - \Omega(2\rho_{ee} - 1). \end{aligned} \quad (6)$$

We then rescale the dimensionful parameters in these equations by letting $t^* = \Gamma t$, $\Omega^* = \frac{\Omega}{\Gamma}$, and $\Delta^* = \frac{\Delta}{\Gamma}$ to obtain the equations used in our numerical solutions:

$$\begin{aligned} \partial_{t^*} \rho_{ee} &= \frac{\Omega^*}{2} \langle \sigma_y \rangle - \rho_{ee} \\ \partial_{t^*} \langle \sigma_x \rangle &= \Delta^* \langle \sigma_y \rangle - \langle \sigma_x \rangle \\ \partial_{t^*} \langle \sigma_y \rangle &= -\Delta^* \langle \sigma_x \rangle - \Omega^*(2\rho_{ee} - 1), \end{aligned} \quad (7)$$

1.2 Data and Results

Numerical solutions to the optical Bloch equations were obtained for the for driving on resonance, $\Delta = 0$, and for large detuning, $\Delta^* = 10$. The numerical results are computed at three different levels of excitation and then plotted for the ground state population.

1.2.1 Driving On Resonance

In this case the analytic solution of the optical Bloch equations has the simple form:

$$\rho_{ee} = \frac{\Omega^2}{2\Omega^2 + \Gamma^2} (1 - e^{-\frac{3}{4}t} (\cos(\Omega_\Gamma t) + \frac{3}{4\Omega_\Gamma} \sin(\Omega_\Gamma t))). \quad (8)$$

For all the different cases, we choose $\rho_e=0$ as the initial condition, tstep=0.01 for the step width and tfinal=10 as final time. For **weak excitation** we set the scaled Rabi frequency $\Omega^*=0.3$ and obtain the following results:

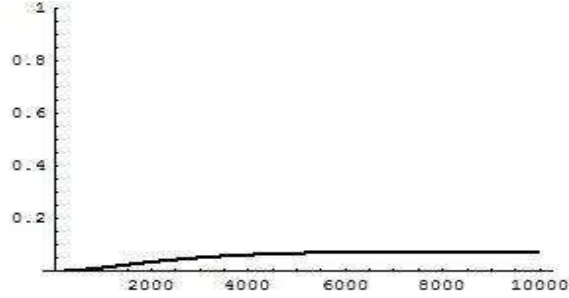


Figure 1: ρ_{ee} vs number of time steps for $\Omega^*=0.3$

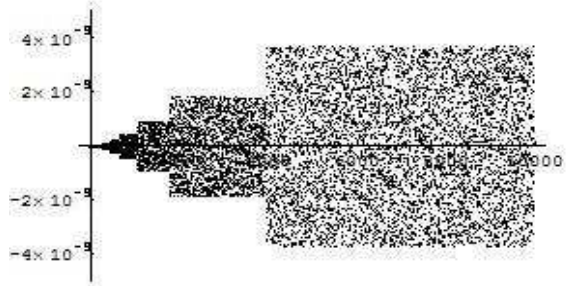


Figure 2: Difference between exact and the numerically determined population vs number of time steps for $\Omega^*=0.3$

Since Ω^* is so small, the atom remains almost entirely in the ground state, no oscillation is observable, and the population never exceeds its steady state value. Plotting the difference between this numerical solution and the exact solution shows that they agree up to an order of 10^{-5} .

For **medium excitation**, which we take to be a scaled Rabi frequency $\Omega^*=1$, the excited state population briefly exceeds its steady state value before decaying rapidly to its steady state value. Comparing the numerical to the analytical solution, we see again, that they agree to order 10^{-8} .

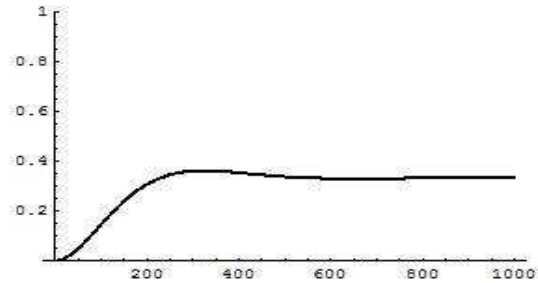


Figure 3: ρ_{ee} vs number of time steps for $\Omega^*=1$

For **strong excitation** we used a scaled Rabi frequency of $\Omega^*=10$. Here we observe Rabi oscillations that slowly damp to the steady state value. Comparison to the exact analytic solution shows that our error is of an order of

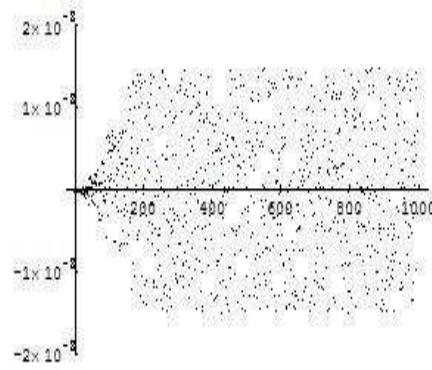


Figure 4: Difference between the exact and the numerically determined population vs number of time steps for $\Omega^*=1$

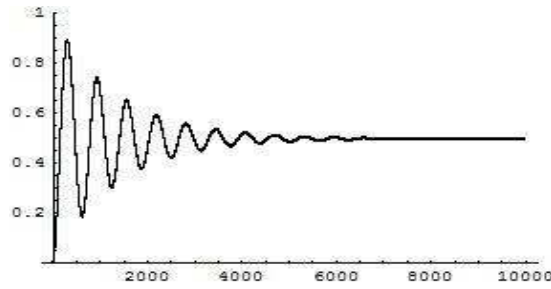


Figure 5: ρ_{ee} vs number of time steps for $\Omega^*=10$

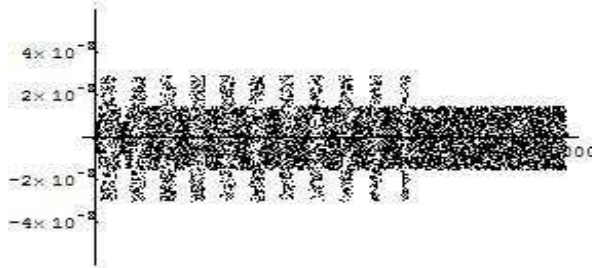


Figure 6: Difference between the exact and numerically determined population vs number of time steps for $\Omega^*=10$

1.3 Driving Off Resonance

A general solution for arbitrary detuning cannot be found in simple form, however in the case of weak driving, $\Omega^* \ll 1$, we can obtain an explicit solution for the excited state population,

$$\rho_{ee} = \frac{\Omega^2}{\Omega^2 + 4\Delta^2} (1 + e^{-\Gamma t} + e^{-\frac{1}{2}\Gamma t} \cos(\Delta t)) \quad (9)$$

which is compared to the numerical results in an error plot for the weak driving cases of $\Omega^* = 0.01$, and $\Omega = 0.1$:

Even for these cases of very weak excitation damped, asymmetrically enveloped oscillations are observed for

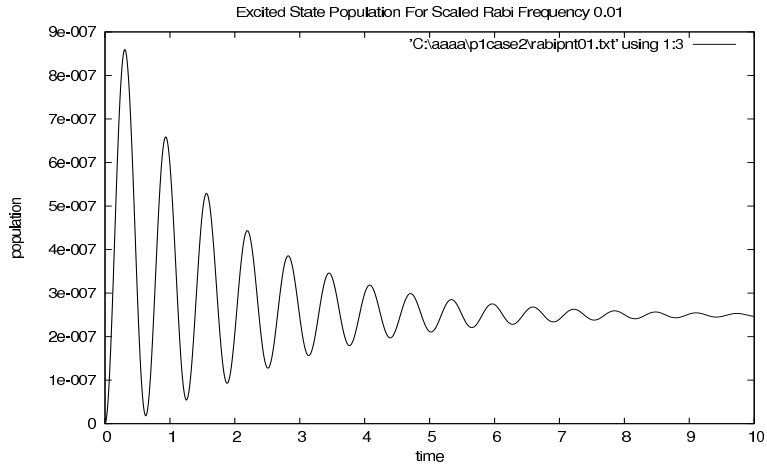


Figure 7: Numerically determined excited state population vs scaled time for $\Omega^*=0.01$

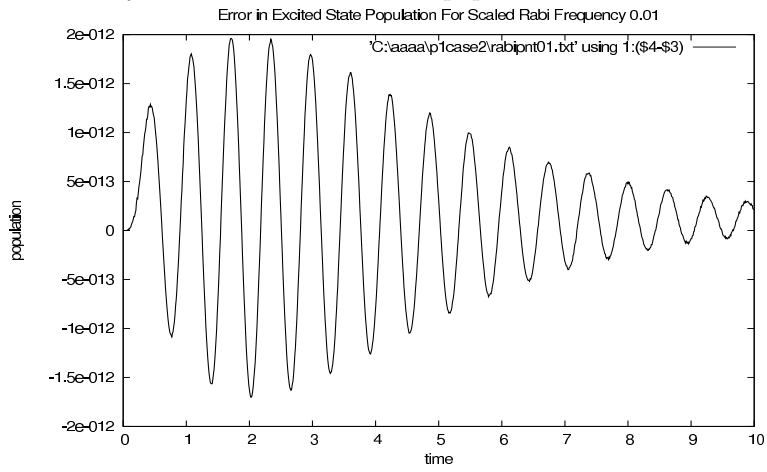


Figure 8: Difference of analytic umerically determined excited state population vs scaled time for $\Omega^*=0.01$

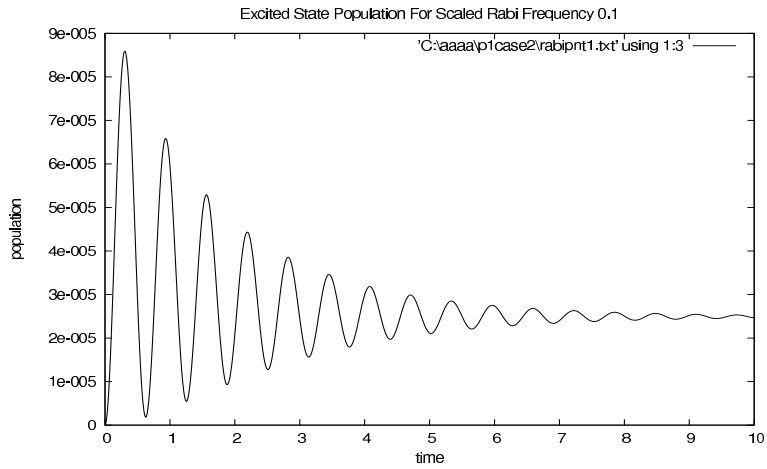


Figure 9: Numerically determined excited state population vs scaled time for $\Omega^*=0.1$

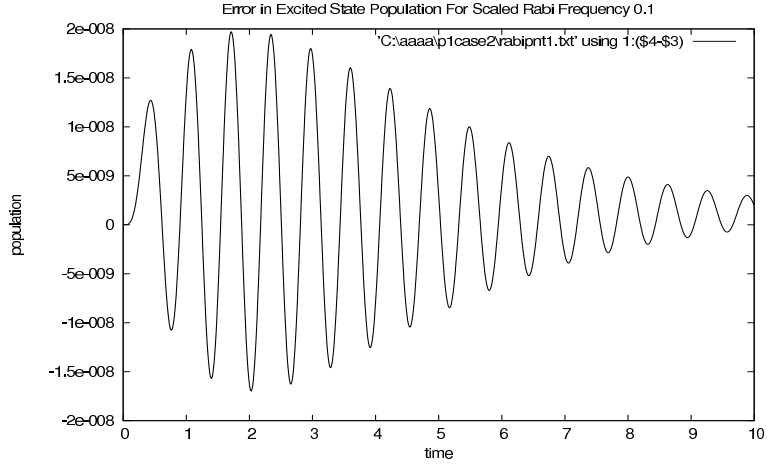


Figure 10: Numerically determined excited state population vs scaled time for $\Omega^*=0.1$

large detunings. The solution remains in very good agreement with the analytically derived result in this regime. Three additional cases with medium, strong, and very strong driving were also investigated for the same detuning. For these the scaled Rabi frequency was taken to be 1, 10, and 100. The general behavior is as expected in these cases, as the amplitude of the Rabi oscillations, and steady state value increases with strong driving. All of the off-resonance numerical solutions were generated using scaled time step size 0.01 and final step 10 except for the very strong driving case, which used a time step of 0.0001 and a final time of 5.

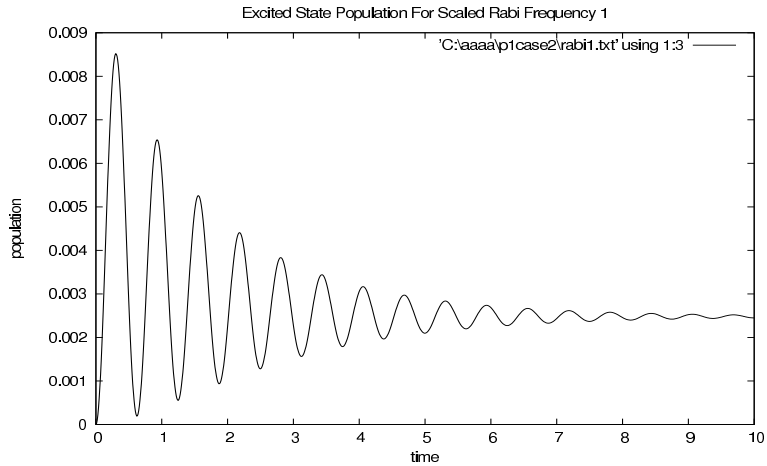


Figure 11: Numerically determined excited state population vs scaled time for $\Omega^*=1$

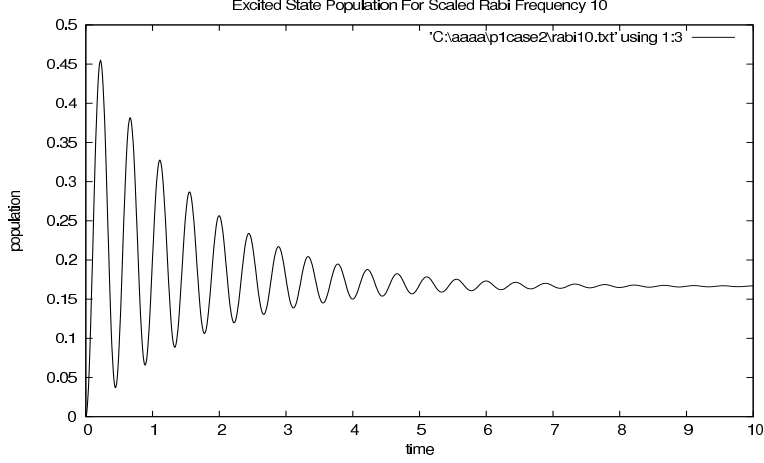


Figure 12: Numerically determined excited state population vs scaled time for $\Omega^*=10$

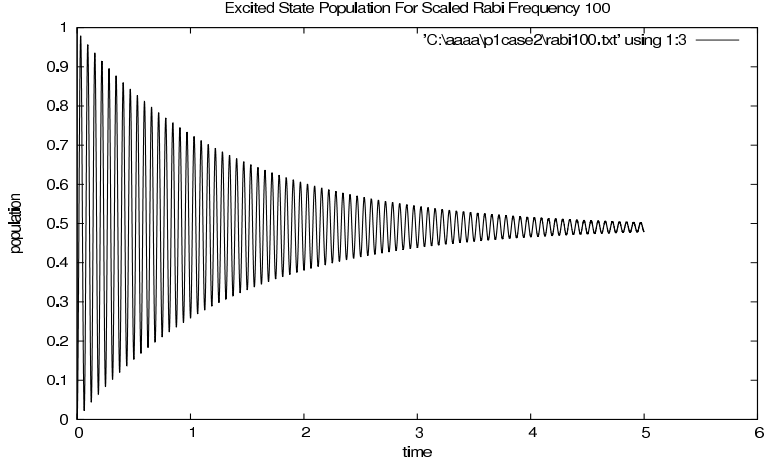


Figure 13: Numerically determined excited state population vs scaled time for $\Omega^*=100$

2 Problem 2

2.1 Theory

In this problem we want to investigate the stochastic master equation. This form of the master equation counts for photon detection. Starting from the stochastic master equation for a two level atom

$$d\rho = -\frac{i}{\hbar} [H_A + H_{AF}, \rho] dt - \frac{\Gamma}{2} [\sigma^\dagger \sigma, \rho]_+ dt + \Gamma \langle \sigma^\dagger \sigma \rangle \rho dt + \left(\frac{\sigma \rho \sigma^\dagger}{\langle \sigma^\dagger \sigma \rangle} - \rho \right) dN, \quad (10)$$

we can show that it simplifies to the much easier unconditioned master equation if we take an ensemble average. dN is defined such that it is unity with probability $\Gamma \langle \sigma^\dagger \sigma \rangle dt$ and zero otherwise for any given time interval dt . Its average can therefore be written as

$$\langle \langle dN \rangle \rangle = \Gamma \langle \sigma^\dagger \sigma \rangle dt. \quad (11)$$

In addition, $\rho(t)$ and $dN(t)$ are statistically independent, such that we can write

$$\langle\langle \rho dN \rangle\rangle = \langle\langle \rho \rangle\rangle \langle\langle dN \rangle\rangle. \quad (12)$$

Using these two restrictions while taking the ensemble average over the stochastic master equation yields to

$$\begin{aligned} d\langle\langle \rho \rangle\rangle &= -\frac{i}{\hbar} [H_A + H_{AF}, \langle\langle \rho \rangle\rangle] dt - \frac{\Gamma}{2} [\langle\langle \sigma^\dagger \sigma \rangle\rangle, \langle\langle \rho \rangle\rangle]_+ dt + \Gamma \langle\sigma^\dagger \sigma \rangle \langle\langle \rho \rangle\rangle dt + \left(\frac{\langle\langle \sigma \sigma^\dagger \rangle\rangle \langle\langle \rho \rangle\rangle}{\langle\sigma^\dagger \sigma \rangle} - \langle\langle \rho \rangle\rangle \right) dN \\ &= -\frac{i}{\hbar} [H, \langle\langle \rho \rangle\rangle] dt - \frac{\Gamma}{2} [\sigma^\dagger \sigma, \langle\langle \rho \rangle\rangle]_+ dt + \Gamma \sigma \langle\langle \rho \rangle\rangle \sigma^\dagger. \end{aligned} \quad (13)$$

The unconditioned master equation describes a measurement process where the actual information from the measurement is not accounted for and the observer takes the average over all possible outcomes (e.g. photon detection, no photon detection).

As we want to do calculations, we would rather deal with the easier Schroedinger equation instead of the master equation. The state vector $|\psi\rangle$ has only $O(n)$ components, while the density matrix has $O(n^2)$ components; the Schroedinger equation is therefore much easier to solve computationally. It shall be shown in the following that the Schroedinger equation is equivalent to the master equation. Therefore we make the assumption to be in a pure state, such that we can write the density operator as

$$\rho = |\psi\rangle \langle\psi|, \quad (14)$$

and obtain by a second order expansion for the differential operator

$$d\rho = d(|\psi\rangle) \langle\psi| + |\psi\rangle d(\langle\psi|) + (d|\psi\rangle) (d\langle\psi|). \quad (15)$$

We start out with the stochastic Schroedinger equation for $d|\psi\rangle$ and $d\langle\psi|$ which leads to

$$\begin{aligned} d|\psi\rangle \langle\psi| &= \left(-\frac{i}{\hbar} H |\psi\rangle dt + \frac{\Gamma}{2} (\langle\sigma^\dagger \sigma \rangle - \sigma^\dagger \sigma) |\psi\rangle dt + \frac{\sigma}{\sqrt{\langle\sigma^\dagger \sigma \rangle}} - 1\right) |\psi\rangle dN \langle\psi| \\ &= -\frac{i}{\hbar} H \rho dt + \frac{\Gamma}{2} (\langle\sigma^\dagger \sigma \rangle - \sigma^\dagger \sigma) \rho dt + \left(\frac{\sigma}{\sqrt{\langle\sigma^\dagger \sigma \rangle}} - 1\right) \rho dN \\ |\psi\rangle d(\langle\psi|) &= \left(\frac{i}{\hbar} H \rho dt + \frac{\Gamma}{2} \rho (\langle\sigma^\dagger \sigma \rangle - \sigma^\dagger \sigma) dt + \rho \left(\frac{\sigma}{\sqrt{\langle\sigma^\dagger \sigma \rangle}} - 1\right) dN\right). \end{aligned} \quad (16)$$

The second order term of the evolution is

$$d|\psi\rangle d\langle\psi| = \frac{\sigma \rho \sigma^\dagger}{\langle\sigma^\dagger \sigma \rangle} dN - \left(\frac{\sigma \rho - \rho \sigma^\dagger}{\sqrt{\langle\sigma^\dagger \sigma \rangle}}\right) dN + \rho dN. \quad (17)$$

Finally combining all these terms recovers the stochastic master equation.

2.2 Computational methods

The stochastic Schroedinger equation cannot be solved directly with a computational integrator, as there are still parts with dt and parts with dN in the equation. Therefore, we have to find a different way to

account for the stochastic parts. We include them in the code as follows: First, we integrated the equations of motion from t to $t+\Delta t$ under the assumption that $dN=0$ during this time interval. Then we account for the stochastic part by introducing randomness to the system. After each time step we pick a random number $\zeta \in [0,1)$ and compared it to

$$\Delta N = \Gamma \frac{\langle \sigma^\dagger \sigma \rangle (t) + \langle \sigma^\dagger \sigma \rangle (t + \Delta t)}{2} \Delta t. \quad (18)$$

If $\zeta \leq 0$ a photon was detected. We change the state then to the ground state. For $\zeta \geq 0$ we don't do anything as the correct solution at time $t+\Delta t$ is already obtained. This process is applied to every time step until we reach the final time. In this way we account for stochastic processes without directly solving the stochastic master equation.

2.3 Data and Results

To completely characterize all possible solutions we would have to vary the parameters Δ , Γ , $tstep$, and the number of trajectories. Obviously varying all of these parameters for even a small number of different values, such as four different values, and comparing against every other parameter value would give an excessive amount of data and plots, $4^4 = 256$ to be exact. Instead, for parameters not under investigation, the default values of $ntraj=10^4$, $tstep=0.01$, $\Omega=1.0$, $\Delta=0.0$ are used. All figures are of ρ_{ee} versus five time units scaled by Γ .

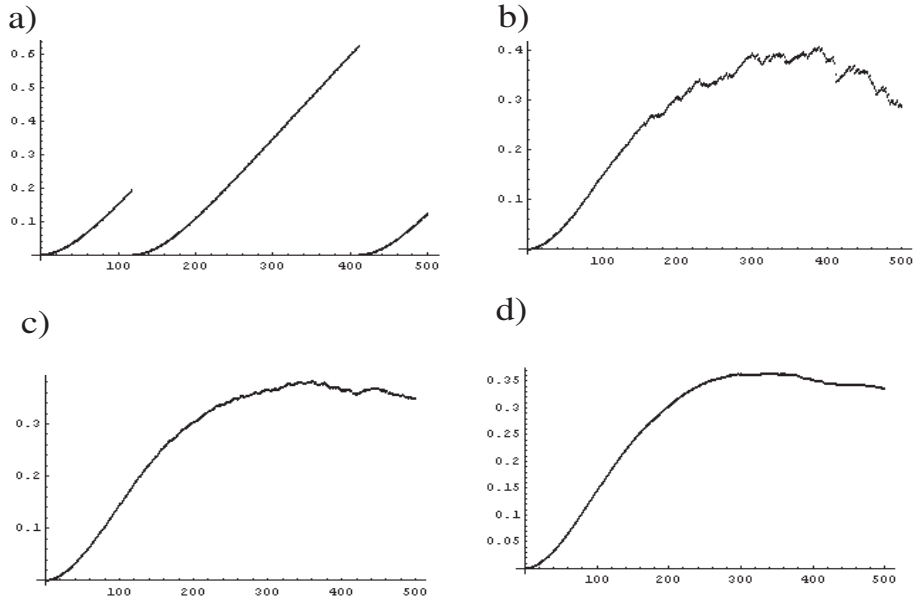


Figure 14: Investigation on the number of trajectories: a)1, b)100, c)1000

First, the number of trajectories averaged over was investigated, with the number varying from 1, 100, 1000 and 10^4 . As can be seen from figure 2.3, the solutions don't converge very well until the number of trajectories is between 1000 and 10^4 . Therefore for all subsequent plots the number of trajectories averaged over will be 10^4 .

Second, the step size was varied from 0.1, 0.01 and 0.001, and the results are shown in figure 18. Clearly the

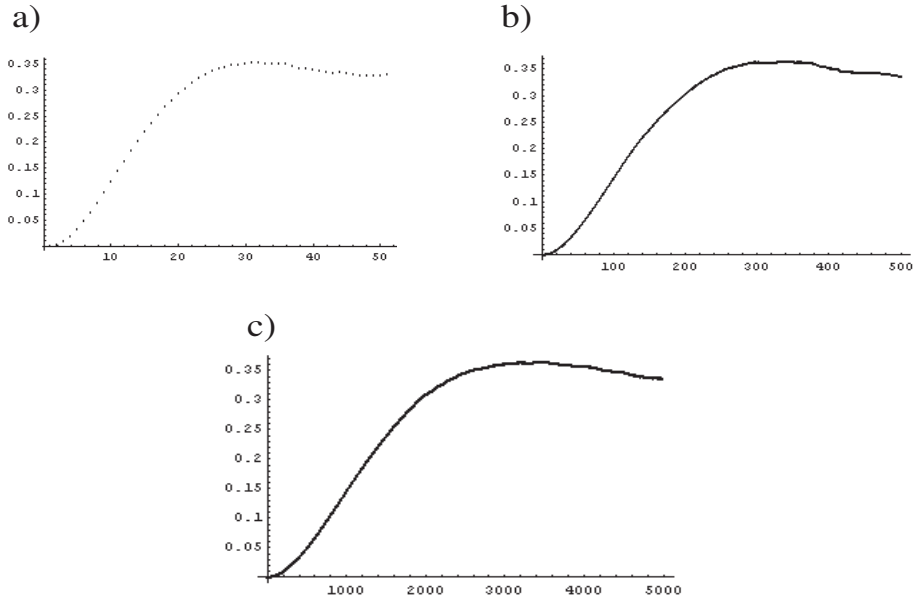


Figure 15: Variation of the step size a) 0.1, b) 0.01, c) 0.001

.1 value does not give good results whereas the 0.01 and 0.001 values do. For all subsequent plots a value of 0.01 will be used for $tstep$.

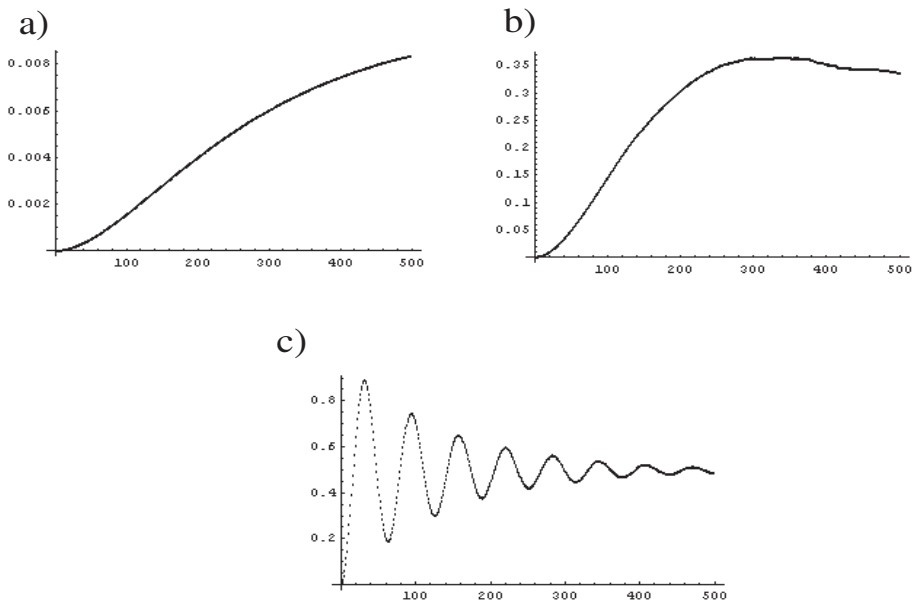


Figure 16: Variation of Ω a) 0.1, b) 1, c) 10

Thirdly, Ω was varied from 0.1, 1 and 10, scaled by Γ , and the results are shown in figure 19. For the small value of Ω , where the driving is not very strong, the solution slowly oscillates, as would be expected since the rabi frequency is small. Also, the excited state population will be small relative to larger values because the damping effects the state before it has much time to grow. For larger values of Ω the oscillations become

more apparent, since the Rabi frequency is larger, and the steady state values of ρ_{ee} are larger as expected.

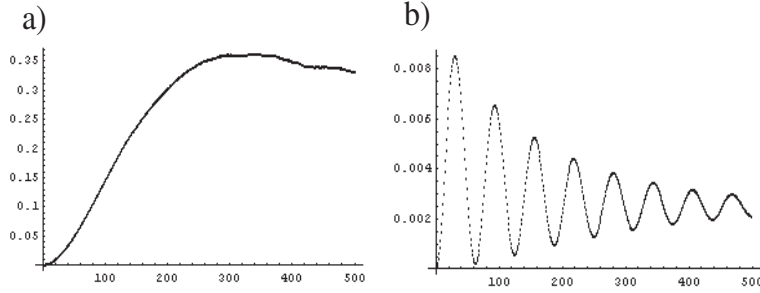


Figure 17: Variation of the detuning a) 0.1, b) 10

Lastly, Δ was varied from 0.1 and 10, scaled by γ , and the results are shown in figure 17. For small Δ there is hardly any change from $\Delta = 0$, which makes sense. For larger Δ there are fast oscillations because the Rabi frequency is large. Interestingly, the excited population is small. Since large Δ is just large detuning (far off resonance) it is expected that not much of the population would be excited, which agrees with the results.

Summing up on our results, we think that they are in good agreement with the theoretical expectations for this problem: for high enough Rabi frequencies we get damped oscillations between the ground and the excited state. The randomness that accounts for the stochastic parts of the equation damps the oscillations until all atoms stay in the ground state.

3 Problem 3

3.1 Theory

For the vee atom one interesting phenomena to observe are Quantum jumps. The transition between Level 1 and Level 2 is weak, while the transition between Level 1 and Level 3 is strongly allowed and strongly driven. Transitions between 2 and 3 are forbidden. Light is scattered from the strong transition while the weak transition still occurs occasionally. To investigate this phenomena, we need to modify the master equation as we did it in problem 2. We will again use the easier Schroedinger equation and include its stochastic parts introducing randomness to the problem.

Since we are treating the vee atom with **indistinguishable decay channels** in this simulation, we can treat the decay process effectively as one single decay process. The transition between the two excited states is forbidden. The modified unconditioned master equation becomes

$$\partial_t \rho = -\frac{i}{\hbar} [H, \rho] + D[\sqrt{\Gamma_1} \sigma_1 + \sqrt{\Gamma_2} \sigma_2] \quad (19)$$

where as usual Γ_1 and Γ_2 are the decay constants for excited states one and two respectively and σ_1 and σ_2 are the lowering operators for excited states one and two respectively.

Motivated by the above master equation we write the stochastic Schrodinger equation similarly to the two level atom except with the substitution that

$$\Gamma \sigma \rightarrow \sqrt{\Gamma_1} \sigma_1 + \sqrt{\Gamma_2} \sigma_2 \quad (20)$$

which yields

$$\begin{aligned}
d|\psi\rangle\langle\psi| = & \left(-\frac{i}{\hbar}H + \left(\frac{\Gamma_1}{2}\langle\sigma_1^\dagger\sigma_1\rangle + \frac{\Gamma_2}{2}\langle\sigma_2^\dagger\sigma_2\rangle + \sqrt{\Gamma_1\Gamma_2}\text{Re}(\langle\sigma_2^\dagger\sigma_1\rangle) \right) \right) |\psi\rangle\langle\psi| dt \\
& + \left(\frac{\Gamma_1}{2}\sigma_1^\dagger\sigma_1 + \frac{\Gamma_2}{2}\sigma_2^\dagger\sigma_2 + \sqrt{\Gamma_1\Gamma_2}\text{Re}(\sigma_2^\dagger\sigma_1) \right) |\psi\rangle\langle\psi| dt \\
& + \left(\frac{\sqrt{\Gamma_1 c_1 + \sqrt{\Gamma_2} c_2}}{2\sqrt{\Gamma_1|c_1|^2 + \Gamma_2|c_2|^2 + \sqrt{\Gamma_1\Gamma_2}\text{Re}[c_2^*c_1]}} \right) |\psi\rangle dN.
\end{aligned} \tag{21}$$

Now, using the common Hamiltonian for the three level atom and invoking the RWA and hitting the left hand side of the equation with $\langle\psi|$ gives

$$\begin{aligned}
dc_g = & \left(-\frac{i}{2}\Omega_1 c_1 - \frac{i}{2}\Omega_2 c_2 + c_g \frac{1}{2}(\Gamma_1|c_1|^2 + \Gamma_2|c_2|^2) + 2\sqrt{\Gamma_1\Gamma_2}\text{Re}[c_2^*c_1] \right) dt \\
& + \left(\frac{\sqrt{\Gamma_1 c_1 + \sqrt{\Gamma_2} c_2}}{2\sqrt{\Gamma_1|c_1|^2 + \Gamma_2|c_2|^2 + \sqrt{\Gamma_1\Gamma_2}\text{Re}[c_2^*c_1]}} \right) dN \\
dc_1 = & \left(i\Delta_1 c_1 - \frac{i}{2}\Omega_1 c_g - \frac{1}{2}\Gamma_1 c_1 - \frac{1}{2}\sqrt{\Gamma_1\Gamma_2} c_2 + c_1 \frac{1}{2}(\Gamma_1|c_1|^2 + \Gamma_2|c_2|^2 + \sqrt{\Gamma_1\Gamma_2} 2\text{Re}[c_2^*c_1]) \right) dt - c_1 dN \\
dc_2 = & \left(i\Delta_2 c_2 - \frac{i}{2}\Omega_2 c_g - \frac{1}{2}\Gamma_2 c_2 - \frac{1}{2}\sqrt{\Gamma_1\Gamma_2} c_1 + c_2 \frac{1}{2}(\Gamma_1|c_1|^2 + \Gamma_2|c_2|^2 + \sqrt{\Gamma_1\Gamma_2} 2\text{Re}[c_2^*c_1]) \right) dt - c_2 dN
\end{aligned} \tag{22}$$

In the scenario of the Quantum Zeno effect, the transition between the first excited state and the ground state is negligible, so for this case we will choose a small Γ_1 and a small Ω_1 for the transition to the first excited state, while Γ_2 and Ω_2 are chosen to be large.

3.2 Methodology

The above equations, similar to problem 2, are not in a form that can be readily solved numerically due to the dN term. Therefore the equations are solved in a similar manner to problem two, except this time ΔN is

$$\Delta N = \langle cc^\dagger cc \rangle \tag{23}$$

where cc is the operator $cc = \sqrt{\Gamma_1}\sigma_1 + \sqrt{\Gamma_2}\sigma_2$. This implies that dN is

$$dN = \overline{\Gamma_1\langle\sigma_1^\dagger\sigma_1\rangle + \Gamma_2\langle\sigma_2^\dagger\sigma_2\rangle + \sqrt{\Gamma_1\Gamma_2}(\langle\sigma_1^\dagger\sigma_2\rangle + \langle\sigma_2^\dagger\sigma_1\rangle)} \tag{24}$$

where the overline signifies a linear time average of the quantity at time t and $t + \Delta t$. Taking the expectation value explicitly we see

$$dN = \overline{\Gamma_1|c_1|^2\Gamma_1|c_2|^2 + \sqrt{\Gamma_1\Gamma_2}2\text{Re}[c_2^*c_1]}. \tag{25}$$

Now we apply an algorithm very similar to the one used in problem 2. First, we integrate the equations of motion from t to $t + \Delta t$ under the assumption that $dN=0$ during this time interval. Then we account for the stochastic part by introducing randomness to the system. After each time step we pick a random number $\zeta \in [0,1)$ and compare it to ΔN . For $\zeta \geq 0$ we don't do anything. For $\zeta \leq 0$ we push the atom to the ground state. This process is applied to every time step until we reach the final time. In this way we account for the measuring.

3.3 Data and results

By calculating the fluorescence spectrum, which is the sum of the populations and coherences weighted by the various Γ s, we can observe Quantum jumps. Since the transition between the first excited state $|e_1\rangle$

and the ground state $|g\rangle$ is weakly damped and weakly driven, the transition between the second excited state $|e_2\rangle$ and $|g\rangle$ is strongly damped and strongly driven, and the transition between the two excited states is forbidden, the main contribution to the spectrum should come from the transition between $|e_2\rangle$ and $|g\rangle$. The weakly driven transition still occurs, which leads to the jumps in the spectrum; the flow of the strongly scattered light is interrupted for the duration of transitions from $|e_1\rangle$. The plot of the scattered intensity over time therefore shows the resonance fluorescence from the strong transition as bright light interrupted by short periods of darkness. Its occurrences and durations are ruled by the corresponding transition rates.

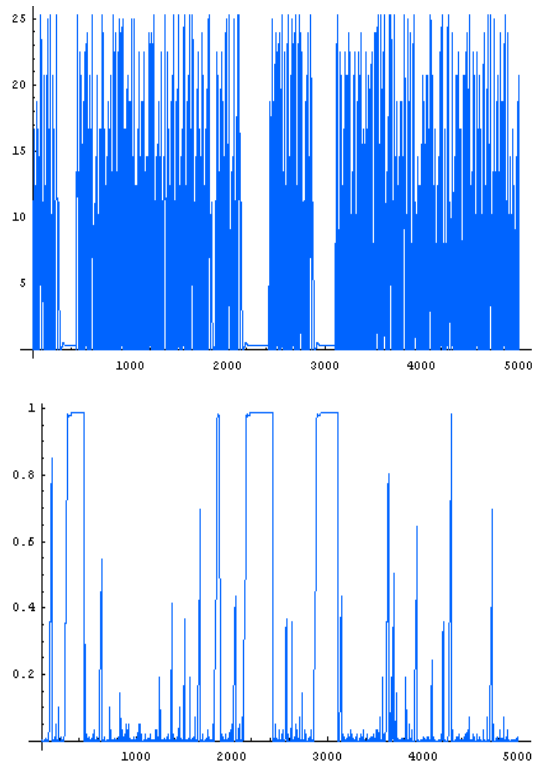


Figure 18: a) Resonance fluorescence as an indicator of quantum jumps. As is shown, when the spectrum is large many transitions between the strongly driven and ground state occur. The "dark state" occurs when population is transferred to the weakly driven state. b) Population of the weakly driven state. As one would expect, the dark state occurs when the population is large and is not immediately collapsed back to the ground state.